



OPEN ACCESS

EDITED BY
 Fakhreddin Jamali,
 University of Alberta, Canada

*CORRESPONDENCE
 Yutaka Inoue,
 ✉ yinoue@josai.ac.jp

RECEIVED 07 May 2024
 ACCEPTED 26 July 2024
 PUBLISHED 13 August 2024

CITATION
 Inoue Y, Yoshino K, Kudo S, Kodama N,
 Moteki H and Kimura M (2024),
 Preparation, solubility, and anti-
 inflammatory effects of a complex of
 diphenylcyclopropenone/ β -
 cyclodextrin derivatives as the
 treatment of alopecia areata.
J. Pharm. Pharm. Sci 27:13230.
 doi: 10.3389/jpps.2024.13230

COPYRIGHT
 © 2024 Inoue, Yoshino, Kudo, Kodama,
 Moteki and Kimura. This is an open-
 access article distributed under the
 terms of the [Creative Commons
 Attribution License \(CC BY\)](https://creativecommons.org/licenses/by/4.0/). The use,
 distribution or reproduction in other
 forums is permitted, provided the
 original author(s) and the copyright
 owner(s) are credited and that the
 original publication in this journal is
 cited, in accordance with accepted
 academic practice. No use, distribution
 or reproduction is permitted which does
 not comply with these terms.

Preparation, solubility, and anti-inflammatory effects of a complex of diphenylcyclopropenone/ β -cyclodextrin derivatives as the treatment of alopecia areata

Yutaka Inoue ^{1*}, Kaede Yoshino¹, Suzu Kudo¹, Nao Kodama¹, Hajime Moteki² and Mitsutoshi Kimura²

¹Laboratory of Nutri-Pharmacotherapeutics Management, Faculty of Pharmacy and Pharmaceutical Sciences, Josai University, Sakado, Japan, ²Laboratory of Clinical Pharmacology, Faculty of Pharmacy and Pharmaceutical Sciences, Josai University, Sakado, Japan

Purpose: To investigate the preparation of inclusion complexes of diphenylcyclopropenone (DPCP)/ β -cyclodextrin (β -CD) derivatives using a three-dimensional (3D) ball mill, and verify the inclusion behavior of the solid dispersion. Additionally, we aimed to investigate the effect of DPCP/ β -CDs complex formation on the spleens of male C57BL/6 mice in terms of anti-inflammatory effects.

Methods: The inclusion complexes of DPCP with β -CD and hydroxypropyl- β -cyclodextrin (HP β CD) were prepared using a 3D ball mill. Powder X-ray diffraction (PXRD) and Fourier-transform infrared spectroscopy (FT-IR) were used to evaluate the solid-state properties. The solubility of the prepared DPCP/ β -CD and HP β CD complexes and the intermolecular interaction between DPCP and β -CD derivatives in solution were assessed using ¹H nuclear magnetic resonance (NMR). Furthermore, the anti-inflammatory effects of DPCPs in the prepared DPCP/CD complexes were investigated using spleens from male C57BL/6 mice, with measurement of interferon gamma (IFN- γ) secretion as an endpoint. Additionally, the protective effects of each drug on NIH-3T3 cells exposed to ultraviolet (UV) irradiation were examined.

Results: Solid-state characterization confirmed the formation of inclusion complexes in the 3D ground mixture (3DGM) (DPCP/ β -CD = 1/1) and 3DGM (DPCP/HP β CD = 1/1) complexes through PXRD and IR analysis. The solubility of 3DGM (DPCP/ β -CD = 1/1) and 3DGM (DPCP/HP β CD = 1/1) was 17.5 μ g/mL and

Abbreviations: 3DGM, 3D ground mixture; AA, Alopecia areata; ATR, attenuated total reflection; CE, Complexation Efficiency; DPCP, diphenylcyclopropenone; FT-IR, Fourier-transform infrared spectroscopy; HP β CD, hydroxypropyl- β -cyclodextrin; IFN- γ , interferon gamma; LPS, lipopolysaccharide; NMR, ¹H nuclear magnetic resonance; PBS, phosphate-buffered saline; PGE, prostaglandin E; PM, physical mixture; PM, physical mixture; PXRD, powder X-ray diffraction; SEM, scanning electron microscope; β -CD, β -cyclodextrin.

58.4 $\mu\text{g}/\text{mL}$, respectively, indicating higher solubility than that of DPCP alone. NMR analysis of 3DGM samples suggested that DPCP/ β -CD and DPCP/HP β CD form inclusion complexes at a molar ratio of 1/1 but with different inclusion modes. Regarding the anti-inflammatory activity of DPCP, 3DGM (DPCP/HP β -CD) showed anti-inflammatory effects at lower doses compared to 3DGM (DPCP/ β -CD) in terms of IFN- γ and NIH-3T3 cells injured by UV irradiation.

Conclusion: We successfully formed inclusion complexes of DPCP/ β -CD and DPCP/HP β CD using the 3D ground mixture method. NMR analysis suggested that DPCP/ β -CD and DPCP/HP β CD form inclusion complexes at a molar ratio of 1/1 but with different inclusion modes. The anti-inflammatory activity of DPCP was more pronounced in 3DGM (DPCP/HP β CD) at lower doses compared to that in 3DGM (DPCP/ β -CD), indicating that the HP β CD derivatives were more effective in enhancing the anti-inflammatory properties of DPCP.

KEYWORDS

diphenylcyclopropenone, ground mixture, inclusion, solid-state, β -cyclodextrin

Introduction

Alopecia areata (AA) is an inflammatory disease with a genetic and immunological basis [1]. It is an autoimmune condition characterized by the expansion of circular hair follicle tissue and the formation of alopecia patches that experience recurring exacerbation and alleviation. Symptoms of AA include the presence of a dense infiltrate of primarily lymphocytes in the perifollicular area. Additionally, there is increased production of interferon gamma (IFN- γ) and interleukin-15 by lymphocytes in the epilation lesions. Furthermore, activation of CD8-positive NKG2D-positive cytotoxic T cells triggers an autoimmunological response targeting autoantigens derived from hair follicles [2, 3].

AA is the most common form of hair loss disorder and significantly impacts the appearance of hair, leading to concerns for patients and a notable decrease in their quality of life. While local steroid injection therapy is the primary treatment for AA, cases with an inadequate response are recommended to undergo local immunotherapy with diphenylcyclopropenone (DPCP) [4].

A study investigating the effectiveness and safety of DPCP, an immunomodulatory treatment, demonstrated a significant correlation between the severity of alopecia and treatment outcomes [5]. However, DPCP presents challenges due to its insolubility in water (solubility: 18.9 $\mu\text{g}/\text{mL}$) and issues related to its preparation and storage methods. Currently, DPCP is stored in light-shielded bottles in clinical settings and dissolved using acetone. Acetone causes skin irritation and is highly volatile, leading to potential changes in DPCP concentration and difficulties in storing diluted solutions [6]. Additionally, there are concerns regarding the exposure of DPCP to individuals involved in the drug preparation process.

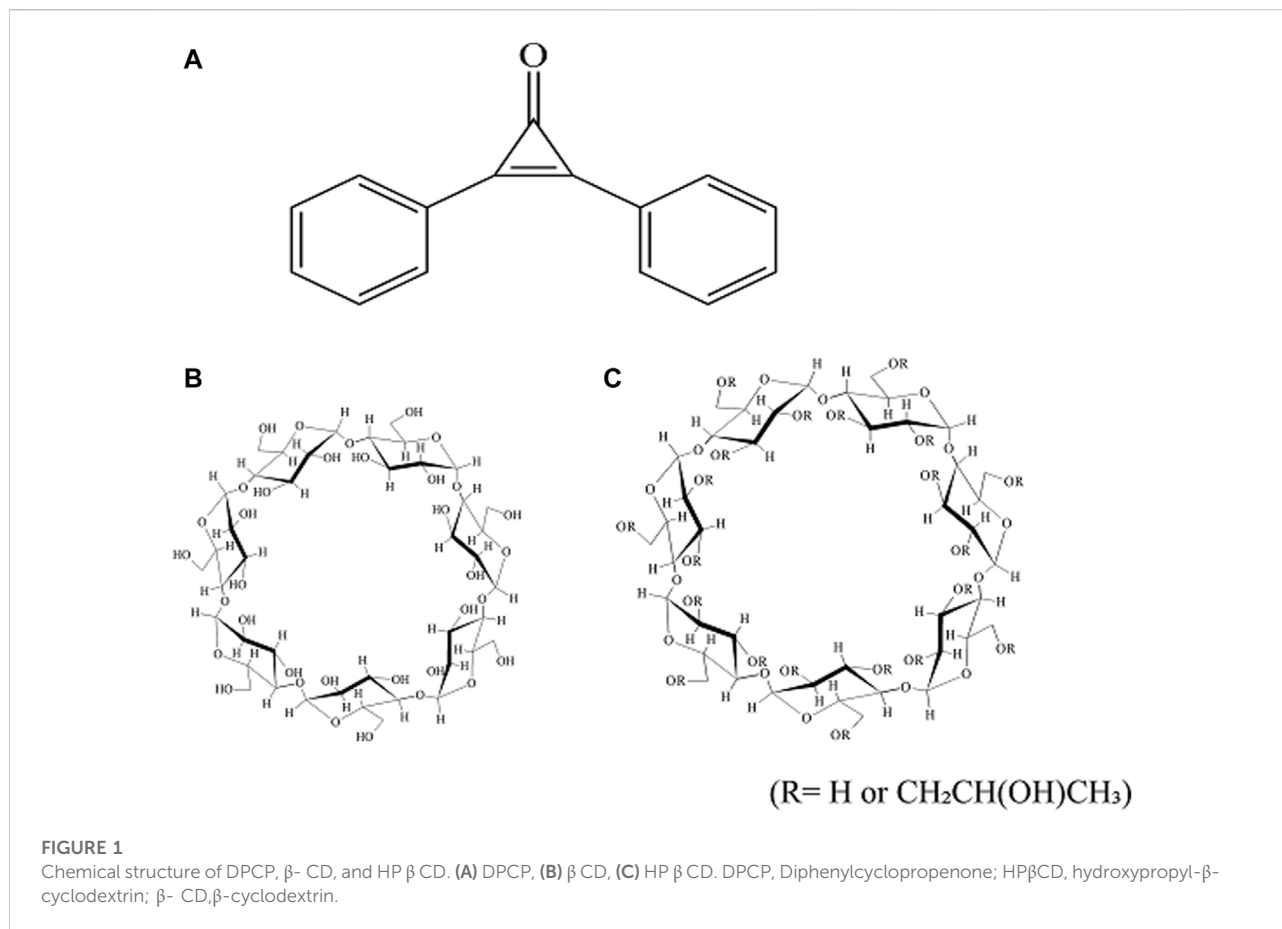
β -cyclodextrin (β -CD) is a naturally occurring cyclic oligosaccharide composed of seven α -D-glucopyranose units linked by $\alpha(1\rightarrow4)$ bonds. It possesses a conical structure with

an outer hydrophilic and an inner hydrophobic region. To enhance its inclusion ability and physicochemical properties, several chemically modified cyclodextrins have been developed. One commonly used non-toxic cyclic oligosaccharide carrier is HP β CD, which is listed as a drug ingredient by the Food and Drug Administration [7]. HP β CD reportedly improves the stability and bioavailability of guest compounds, as well as reduces volatility by providing protection against degradation [8–11].

β -CD can form molecular complexes with various compounds, including prostaglandin E (PGE) [12]. Studies have also demonstrated that paclitaxel complexed with CD exhibits high water solubility and remarkable stability [13]. In the case of hydroxypropyl- β -cyclodextrin (HP β CD), the formation of an inclusion complex with isoflavone compounds reportedly enhances skin permeability [14]. Consequently, there are numerous examples of pharmaceutical applications utilizing β -CD derivatives [15, 16].

Various methods have been reported for the preparation of inclusion complexes, including the coprecipitation method [17], kneading method [18], freeze-drying method [19], and mixing and milling method [20]. One notable complex preparation method is the 3D mixing and milling method, which utilizes a 3D ball mill, a novel milling technique that has gained attention in recent years. The 3D ball mill features two rotary axes, one vertical and one horizontal, and utilizes the entire inner surface of a spherical container. This design reduces frictional heat generation and enables highly uniform milling and mixing in a short time [21].

In our previous work, we reported improved complex formation, solubility, and antioxidant capacity by using the 3D ball-milling technique to prepare mixtures of CDs with aglyconic isoflavones, specifically daidzein and genistein in the context of soy isoflavones [22]. Based on these findings, we



propose that the preparation of inclusion complexes of DPCP with CDs using this innovative ground mixture technique could enhance the solubility of DPCP in the treatment of AA. This approach would allow for the preparation of DPCP at the time of use without the need for organic solvents, such as acetone.

Furthermore, the development of new formulations that consider factors, such as patient skin irritation during treatment, could serve as a foundation for future clinical applications. This method could potentially improve patient comfort and compliance, reduce the risk of adverse reactions, and streamline the preparation and storage of DPCP solutions.

In this study, our objective was to enhance the solubility and anti-inflammatory effects of DPCP, focusing on its inclusion complexes with β -CD and HP β CD using the 3D ball milling method. The solid-state properties of the complexes were evaluated using techniques such as powder X-ray diffraction (PXRD), Fourier-transform infrared spectroscopy (FT-IR), and scanning electron microscope (SEM). Additionally, the solubility and intermolecular interactions were assessed using ^1H nuclear magnetic resonance (NMR) to gain insights into the solubility and interactions between the components.

The anti-inflammatory effects of DPCP in the prepared DPCP/CD complexes were investigated by culturing the

spleens of male C57BL/6 mice and measuring IFN- γ levels in the culture medium. Furthermore, the protective effects of each drug on NIH-3T3 cells, which were injured by ultraviolet (UV) irradiation, were examined.

Materials and methods

Materials

DPCP (Lot No. LEH3622) was purchased from Fujifilm Wako Pure Chemical Corporation (Tokyo, Japan) (Figure 1). β -CD was supplied by Cyclo Chem Co., Ltd. (Kobe, Japan) and stored at 40°C with 82% relative humidity for 7 days. All other reagents used, including those for NMR analysis, were obtained from Fujifilm Wako Pure Chemical Corporation.

Sample preparation of physical mixture and mixed pulverized material

Physical mixtures (PMs) were prepared by weighing the components at a molar ratio of 1/1 and mixing them using a

vortex mixer for 1 min. To prepare 3D ground mixtures (3DGMs), 500 mg of the PM (DPCP/ β -CD, DPCP/HP β CD) was weighed and placed in a grinding cell along with 96 g of Φ 5 mm alumina balls. Then, the mixtures were processed using a 3D ball mill (3D-80, Nagao system Inc., Kawasaki, Japan) for 30 min.

Phase solubility diagrams

A solubility phase diagram was constructed following the method described by Higuchi et al. [23]. Excess DPCP (10 mg) was added to aqueous solutions (10 mL) of varying β -CD (0–50 mM) and HP β CD (0–10 mM) concentrations. The mixtures were shaken ($25 \pm 0.5^\circ\text{C}$) at 100 rpm for 24 h to obtain a suspension. The suspension was filtered through a 0.20- μm membrane filter (Advantec[®], Tokyo, Japan), and the filtrate was quantified by high-performance liquid chromatography (HPLC).

The stability constant (K_s) was calculated from the slope of the solubility phase diagram and the solubility (S_0) of DPCP in the absence of β -CD or HP β CD using the following equation (Eq. 1).

$$K_s = \text{slope}/S_0 \cdot (1-\text{slope}) \quad (1)$$

The complexation efficiency (CE) was calculated using the following equation (Eq. 2).

$$\text{CE} = S_0 \cdot K_s = \text{slope}/(1-\text{slope}) \quad (2)$$

HPLC conditions

Samples were quantified using HPLC (LC-20ADvp, Shimadzu Corp., Kyoto, Japan). The detection wavelength was set at 293 nm. An Inertsil ODS-3 column (4.6×150 mm, Φ 5 μm ; GL Sciences, Tokyo, Japan) was utilized, with a sample injection volume of 10 μL and a column temperature of 40°C . The mobile phase consisted of acetonitrile and water in a 6:4 ratio. The retention time for DPCP was set at 7 min.

PXRD measurement

Diffraction intensities were measured using a NaI scintillation counter on a Miniflex II powder X-ray diffractometer (Rigaku Corporation, Tokyo, Japan). Cu-rays (30 kV, 15 mA) were used as the X-ray source. The X-ray diffraction measurements were conducted at a scan speed of $4^\circ/\text{min}$ over a scan range of $2\theta = 5\text{--}40^\circ$. The powder samples were placed flat on a glass plate for measurement.

FT-IR spectroscopy

Measurements were performed using the attenuated total reflection (ATR) method with a JASCO FT/IR-4600 instrument (JASCO Corporation, Tokyo, Japan). The measurement conditions were as follows: integration frequency, 16; resolution, 4 cm^{-1} ; and measurement range, $400\text{--}4,000\text{ cm}^{-1}$.

Scanning electron microscope (SEM) measurements

A field-emission SEM (JSM-IT800, Schottky Field Emission Scanning Electron Microscope, JOEL Ltd., Tokyo, Japan) was used. Each sample was coated with a thin layer of gold for 60 s to enhance conductivity and observed under a pressurized voltage of 1 kV.

Dissolution test

The dissolution test was conducted using a dissolution tester (NTR-593, Toyama Sangyo, Osaka, Japan) in accordance with the JP18 revised paddle method. The dissolution medium consisted of 300 mL of distilled water maintained at $37 \pm 0.5^\circ\text{C}$, with stirring at 50 rpm. DPCP (50 mg) was placed in a paddle. Samples of 10 mL were collected at 5, 10, 15, 60, and 120 min and, then, filtered through a 0.20- μm membrane filter (DISMIC 25AS, Advantec[®]). To maintain a constant volume of dissolved solution, distilled water (10 mL) was added at the same temperature and volume after each sample collection. The obtained filtrates were diluted with a mixture of acetonitrile and distilled water (6/4), and subsequently analyzed using HPLC.

ROESY NMR and NOESY NMR measurements

An AVANCE NEO 600 NMR system (Bruker, Billerica, MA, United States) was used. Deuterium oxide (D_2O) was employed as the solvent, and the measurement conditions were as follows: resonance frequency, 600.13 MHz; measurement temperature, 25°C ; integration frequency, 32; pulse width, 90° ; and waiting time, 3 s (ROE) and 4 s (NOE).

Isolation and culture of spleen cells

The spleen was removed from a male C57BL/6 mouse (Tokyo Laboratory Animals Science Co., Ltd., Tokyo, Japan), minced with scissors, and filtered through a 55- μm mesh. Thereafter, the cells were hemolyzed using a red blood cell

lysis buffer (Pluriselect-USA Inc., CA, United States) and resuspended in RPMI 1640 medium (Sigma-Aldrich Co., St. Louis, MO, United States) by centrifugation. Isolated splenocytes were confirmed to have >98% viability using trypan blue exclusion assay. Splenocytes (5.0×10^6 cells/mL) were plated and cultured for 48 h in RPMI 1640 medium containing 5% fetal calf serum (GE Healthcare Lifesciences, Inc., IL, United States), 0.01 $\mu\text{g}/\text{mL}$ lipopolysaccharide (LPS) (Sigma-Aldrich Co.), and various reagents. The reagents added to splenocytes were CPDP, HP β CD/CPDP, and β -CD/CPDP.

Measurement of IFN- γ in the culture medium

The IFN- γ concentration in the culture medium (100 μL) was quantified using an ELISA kit (Proteintech Inc., Rosemont, IL, United States), following the manufacturer's instructions. After treating the culture medium with various reagents for 48 h in primary cultures of splenocytes, the samples were collected and centrifuged at $500 \times g$ for 5 min to remove any particulate matter. Subsequently, the supernatant (100 μL) was used for the quantification of IFN- γ concentration.

NIH-3T3 cell culture

NIH3T3 (NIH3T3/14-1) mouse fibroblast cells were obtained from Riken BioResource Center (Ibaragi, Japan) and maintained in Dulbecco's modified eagle medium (DMEM) supplemented with 10% fetal bovine serum and buffered with 44 mM NaHCO_3 at 37°C in a 5% CO_2 incubator [24].

For cell injury experiments, a cell suspension was prepared in the aforementioned medium to a concentration of 1.2×10^3 viable cells/mL. Then, 2 mL of the suspension was seeded onto a 35-mm- ϕ six-well plate (2.5×10^2 viable cells/ cm^2). The cells were cultured in a CO_2 incubator at 37°C with 5% CO_2 for 96 h. To quantify PGE_2 concentration in the culture medium, cells were prepared similarly at a concentration of 1.0×10^2 viable cells/mL and, then, seeded in 2-mL portions (2.5×10^2 viable cells/ cm^2) and cultured for 96 h under the same conditions.

Cell injury experiment

After adding 2 mL of phosphate-buffered saline (PBS) (–) to the NIH-3T3 cells, the dish was irradiated with UV rays from the bottom for 10 s using an 8-m W/cm^2 , 254-nm UV lamp (15 W \times 6). Immediately after UV irradiation, PBS (–) with 2.5 mM glucose and 0.9 mM CaCl_2 was added. The

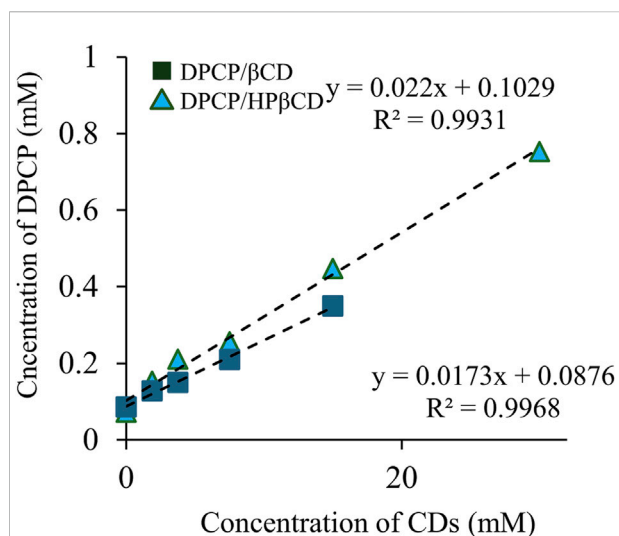


FIGURE 2
Phase solubility diagram of DPCP/ β -CD, DPCP/HP β CD. Results are presented as means \pm standard deviations ($n = 3$). ■ DPCP/ β -CD, ▲ DPCP/HP β CD. DPCP, Diphenylcyclopropanone; HP β CD, hydroxypropyl- β -cyclodextrin; β -CD, β -cyclodextrin.

solution was removed by suction and replaced with the conditioning culture medium (PBS (–) with 2.5 mM glucose and 0.9 mM CaCl_2) to which each drug had been added. The cells were subsequently cultured in a CO_2 incubator (37°C , 5% CO_2) for 4 h [25].

Quantification of PGE_2 concentration

After adding each drug (to the UV-irradiated NIH-3T3 cells and culturing for 4 h, 50 μL of the conditioning culture medium was sampled from each dish. The concentration of PGE_2 in the culture medium was measured using an EIA kit (Arbor Assays, Ann Arbor, MI, United States). The PGE_2 levels were determined colorimetrically at 450 nm. The control groups consisted of cells subjected to UV irradiation without the addition of any drugs, as well as cells without UV irradiation and without drug treatment [26].

Statistical analysis

The results are presented as means \pm standard error of the mean from 3-4 separate experiments for pharmacological measurements. Statistical comparisons between the control and treatment groups were performed using Student's t-test, with significance set at $P < 0.05$. The statistical analysis was conducted using Statcel-the Useful Addin Forms on Excel (fourth edition; OMS Publishing, Tokyo, Japan).

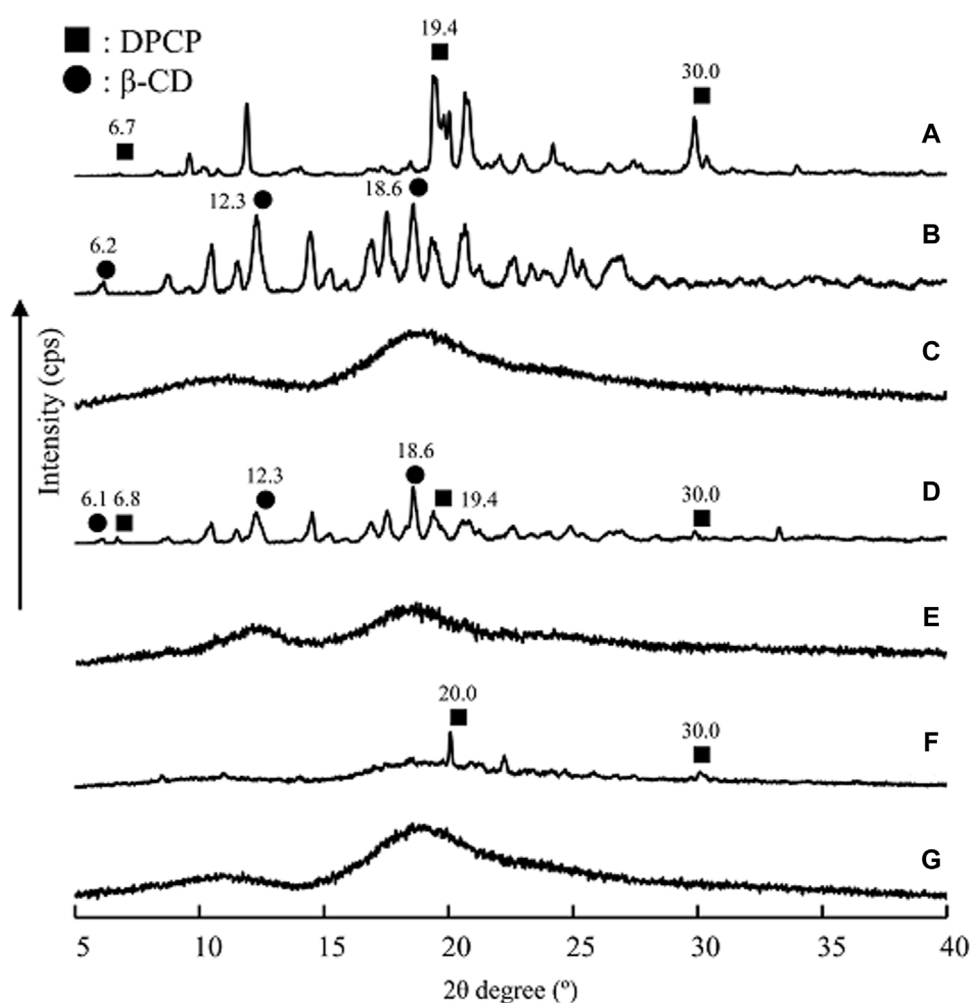


FIGURE 3

PXRD patterns of DPCP intact, DPCP/ β -CD and DPCP/HP β CD systems. (A) DPCP intact, (B) β -CD intact, (C) PM (DPCP/ β -CD = 1/1), (D) 3DGM (DPCP/ β -CD = 1/1), (E) HP β CD intact, (F) PM (DPCP/HP β CD = 1/1), (G) 3DGM (DPCP/HP β CD = 1/1) ■: DPCP original, ▲: β -CD original. 3DGM, three-dimensional ground mixture; DPCP, diphenylcyclopropanone; HP β CD, hydroxypropyl- β -cyclodextrin; PM, physical mixtures; PXRD, Powder X-ray diffraction; β -CD, β -cyclodextrin.

Ethics approval

This study was approved by the Institutional Animal Care and Use Committee of the Josai University (No. JU 22037). All procedures involving animals were conducted in accordance with the regulations outlined in the Josai University Guidelines for the Care and Use of Laboratory Animals.

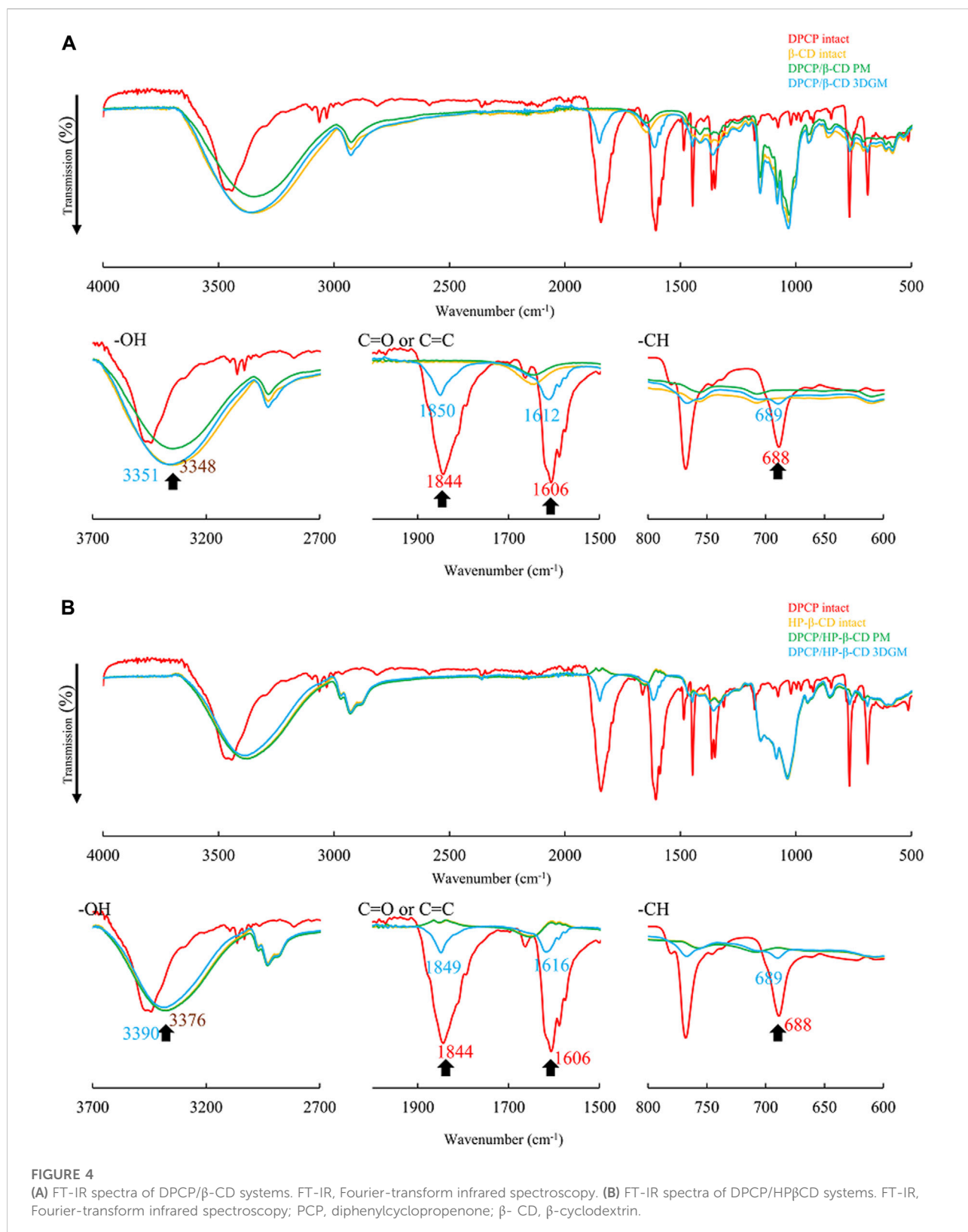
Results and discussion

Solubility phase diagram

Solubility phase diagrams were constructed to analyze the solubility changes of DPCP/ β -CD and DPCP/HP β CD inclusion

complexes in solution, which allowed for the calculation of stability constants and prediction of inclusion molar ratios (Figure 2). According to the classification of solubility phase diagrams, they can be categorized into type A (soluble complexes) and type B (insoluble complexes). Type A includes AL (linear diagram), Ap (positive deviation from linearity), and AN (negative deviation from linearity) types, while type B includes BS (the complex has some but limited solubility) and BI (the complex is insoluble) types [27].

DPCP/ β -CD, the solubility phase diagram, exhibited a linear AL-type relationship, proportional to the increase in β -CD concentration. The K_s was calculated to be 200.4 M^{-1} , with a complexation efficiency (CE) of 1.8×10^{-2} . Similarly, the DPCP/HP β CD solubility phase diagram also showed an AL-type linear relationship, indicating an increase in DPCP solubility



proportional to the HP β CD concentration. The K_s for DPCP/HP β CD was calculated to be 233.5 M^{-1} , with a CE of 2.3×10^{-2} .

The results from the solubility phase diagrams indicate that both DPCP/ β -CD and DPCP/HP β CD form linear AL-type complexes as per the Higuchi et al. classification, suggesting a 1/1 inclusion molar ratio in solution. The higher stability constant for DPCP/HP β CD compared to DPCP/ β -CD suggests that DPCP has a greater tendency to form a complex with HP β CD than with β -CD.

PXRD measurement

The researchers conducted PXRD measurements to examine changes in the crystalline state of solid dispersions of DPCP/ β -CD and DPCP/HP β CD that were prepared using 3D milling (Figure 3). Characteristic diffraction peaks for DPCP were observed at $2\theta = 6.7^\circ$, 19.4° , and 30.0° , while β -CD exhibited characteristic peaks at $2\theta = 12.3^\circ$ and 18.6° . HP β CD displayed a halo pattern without any characteristic diffraction peaks.

For the DPCP/ β -CD solid dispersion prepared by physical mixing (PM), both DPCP and β -CD peaks were observed. However, in the 3DGM of DPCP/ β -CD, the peaks from DPCP and β -CD disappeared, and a halo pattern was observed. Similarly, in the DPCP/HP β CD solid dispersion PM, the DPCP-derived peak was present, but in the 3DGM of DPCP/HP β CD, both the DPCP- and β -CD-derived peaks disappeared, resulting in a halo pattern.

Previous studies have reported that co-milling can disrupt the crystalline structure, leading to the formation of amorphous solids that exhibit a halo pattern [28]. It has also been suggested that mechanical energy applied during milling and friction can contribute to the formation of amorphous inclusion complexes [29]. Based on the PXRD results, the characteristic diffraction peaks of DPCP, β -CD, and HP β CD were not observed, indicating the formation of inclusion complexes with a presumed molar ratio of 1/1 in the 3DGM of DPCP/ β -CD and DPCP/HP β CD.

FT-IR spectroscopy

The PXRD results suggested that DPCP/ β -CD and DPCP/HP β CD in the solid state form inclusion complexes with a DPCP/CD molar ratio of 1:1. To further confirm the intermolecular interactions within these complexes, FT-IR absorption spectroscopy was conducted (Figure 4). For DPCP, the FT-IR spectrum exhibited characteristic peaks at 688 cm^{-1} for the -CH group derived from the aromatic ring, $1,606 \text{ cm}^{-1}$ for C=C, and $1,844 \text{ cm}^{-1}$ for the ketone group.

In the physical mixtures (PMs) of DPCP/ β -CD and DPCP/HP β CD, the original peaks derived from DPCP and β -CD were observed (Figure 4A). However, in the 3DGM of DPCP/ β -CD, shifts were observed in the DPCP-derived peaks: the -CH group

peak shifted to 689 cm^{-1} , the C=C peak to $1,612 \text{ cm}^{-1}$, and the ketone group peak to $1,850 \text{ cm}^{-1}$. Similarly, in the 3DGM of DPCP/HP β CD, the -CH group peak shifted to 689 cm^{-1} , the C=C peak to $1,616 \text{ cm}^{-1}$, and the ketone group peak to $1,849 \text{ cm}^{-1}$ (Figure 4B).

Additionally, in the 3DGM samples, the peaks around $3,348 \text{ cm}^{-1}$ for β -CD and $3,376 \text{ cm}^{-1}$ for HP β CD, which correspond to the -OH groups, shifted to $3,351 \text{ cm}^{-1}$ and $3,390 \text{ cm}^{-1}$, respectively. The shifts in these peaks, which are attributed to DPCP and β -CD alone, suggest the formation of intermolecular interactions between the C=O and C=C groups of DPCP, the aromatic ring -CH, and the -OH groups of β -CD. These interactions confirm the inclusion complex formation in the solid state through mixed grinding.

SEM measurements

In the solid state, 3DGMs of DPCP/ β -CD and DPCP/HP β CD, both with a 1:1 M ratio, were suggested to form inclusion complexes. PXRD measurements indicated changes in the crystal state of these complexes. To evaluate the microstructure and surface morphology of the prepared inclusion complexes, SEM measurements were performed. SEM, with its high resolution, can observe fine structures on the nanometer scale, providing detailed insights into the microstructure and surface characteristics of the materials (Figure 5).

The SEM images revealed that the crystal surface of intact DPCP appeared smooth and columnar, with particle sizes around $100 \mu\text{m}$ (Figure 5A). Intact β -CD displayed a smooth and angular crystal surface with particle sizes around $150 \mu\text{m}$ (Figure 5B). In the PM of DPCP/ β -CD (1/1), no significant changes in the particle surfaces of DPCP and β -CD were observed (Figure 5C).

Generally, when β -CD forms inclusion complexes, cubic crystals are reported to appear. In the 3DGM of DPCP/ β -CD (1/1), the particle size was reduced to around $100 \mu\text{m}$ due to milling, and the particles exhibited a cubic shape with fine surface attachments, suggesting the formation of an inclusion complex (Figure 5D).

HP β CD intact exhibited a smooth and spherical crystal surface with particle sizes around $100 \mu\text{m}$ (Figure 5E). In the PM of DPCP/HP β CD (1/1), the particle surfaces of DPCP and HP β CD remained unchanged (Figure 5F). Typically, when HP β CD forms inclusion complexes, crystals with a folded structure are observed [30]. In the 3DGM of DPCP/HP β CD (1/1), the particle size was further reduced to approximately $30 \mu\text{m}$, and a plate-like folded structure with fine particles on the surface was observed, indicating the formation of an inclusion complex (Figure 5G).

These SEM observations suggest that the particle shapes and surface morphologies changed due to the formation of inclusion

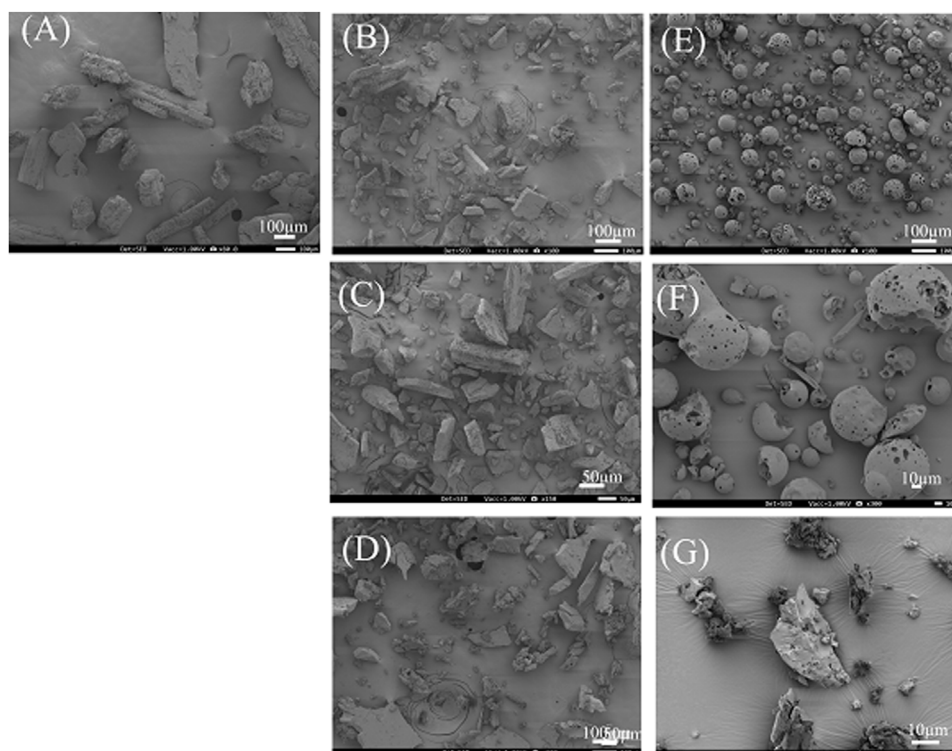


FIGURE 5

SEM image of DPCP/β-CD, DPCP/HPβCD systems. (A) DPCP intact, (B) β-CD intact, (C) PM (DPCP/β-CD = 1/1), (D) 3DGM (DPCP/β-CD = 1/1), (E) HPβCD intact, (F) PM (DPCP/HPβCD = 1/1), (G) 3DGM (DPCP/HPβCD = 1/1) 3DGM, three-dimensional ground mixture; DPCP, diphenylcyclopropanone; HPβCD, hydroxypropyl-β-cyclodextrin; PM3DGM, three-dimensional ground mixture, physical mixtures; PXRD, Powder X-ray diffraction; β-CD, β-cyclodextrin.

complexes through the 3DGM process, confirming the successful inclusion of DPCP with β-CD and HPβCD.

Dissolution test

Solid-state characterization confirmed the formation of inclusion complexes in 3DGMs of DPCP/β-CD (1/1) and DPCP/HPβCD (1/1). To further investigate the change in solubility of DPCP with each inclusion complex, dissolution tests were conducted using samples of intact DPCP, 3DGM (DPCP/β-CD = 1/1), and 3DGM (DPCP/HPβCD = 1/1) (Figure 6).

Initially, the dissolution concentration of intact DPCP at 15 min was measured at 5.70 μg/mL. In contrast, both 3DGM (DPCP/β-CD = 1/1) and 3DGM (DPCP/HPβCD = 1/1) exhibited faster dissolution of DPCP compared to DPCP alone, with concentrations measured at 17.5 μg/mL and 58.4 μg/mL, respectively, from study initiation. This significant increase in the solubility of DPCP in the presence of inclusion complexes can be attributed to two main factors: the formation of inclusion complexes between DPCP and β-CD or HPβCD, and

the increase in specific surface area due to the smaller particle size achieved through milling.

Notably, the solubility of DPCP was higher in 3DGM (DPCP/HPβCD = 1/1) compared to that in 3DGM (DPCP/β-CD = 1/1). This suggests that there may be differences in the inclusion mode or interaction strength between DPCP/β-CD and DPCP/HPβCD complexes, in addition to the findings from the physical properties evaluation in the solid state.

ROESY NMR and NOESY NMR measurements

NMR spectroscopy was employed to elucidate the inclusion modes of DPCP with β-CD and HPβCD in the prepared 3DGM at a 1:1 mole ratio. In the case of 3DGM (DPCP/β-CD = 1/1), cross-peaks were identified between the -CH (A; 7.94 ppm) of DPCP and the -OH groups of β-CD (H-6; 3.71 ppm, H-3; 3.82 ppm), as well as between -CH (B; 7.55 ppm) of DPCP and -OH (H-6; 3.71 ppm) of β-CD (Figure 7A) [31–33]. These findings indicate that DPCP is encapsulated by β-CD from the

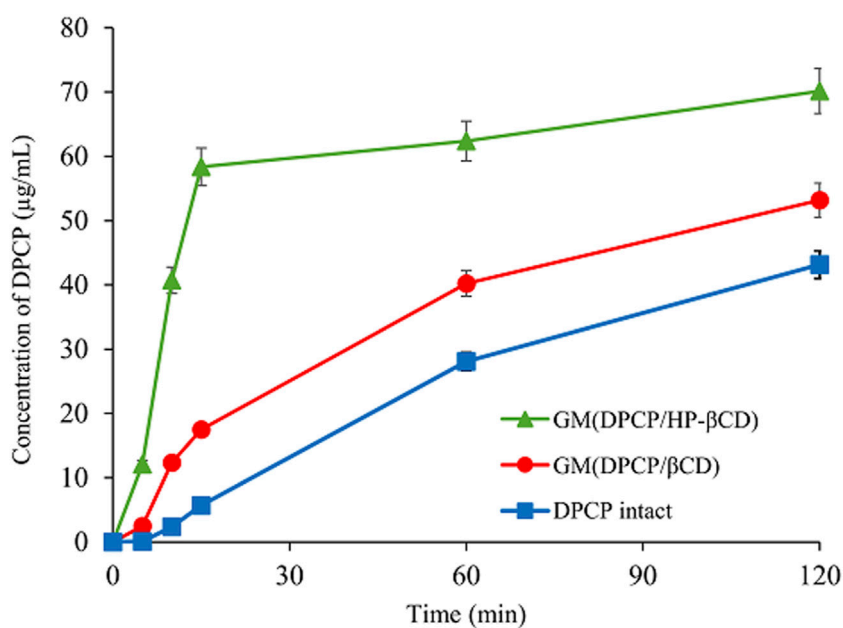


FIGURE 6

Dissolution profiles of DPCP intact, DPCP/β-CD and DPCP/HPβCD systems. Results are presented means ± standard deviations (n = 3). DPCP, diphenylcyclopropanone; HPβCD, hydroxypropyl-β-cyclodextrin; β-CD, β-cyclodextrin.

wide edge (H-3) to the narrow edge (H-6), encompassing the benzene ring of DPCP.

Conversely, in 3DGM (DPCP/HPβCD = 1/1), cross-peaks were observed between -CH of DPCP (A; 7.95 ppm) and -OH of HPβCD (H-6; 3.72 ppm), as well as between -CH (B; 7.55 ppm) of DPCP and -OH (H-6; 3.72 ppm) of HPβCD (Figure 7B). These results from ROESY and NOESY NMR measurements suggest that HPβCD encapsulates DPCP such that the CD surrounds the benzene ring of DPCP from the narrow edge (H-6) to the wide edge (H-3).

The distinct cross-peak patterns observed in the NMR spectra of DPCP/β-CD and DPCP/HPβCD complexes indicate different inclusion modes between DPCP and the CDs in solution. Specifically, DPCP/β-CD predominantly interacts with the -OH groups of β-CD, while DPCP/HPβCD interacts in a manner where HPβCD surrounds the benzene ring of DPCP.

These findings further support the hypothesis that the 3DGM preparation method affects the inclusion mode and interaction strength of DPCP with β-CD and HPβCD, influencing their solubility enhancement properties observed in dissolution tests.

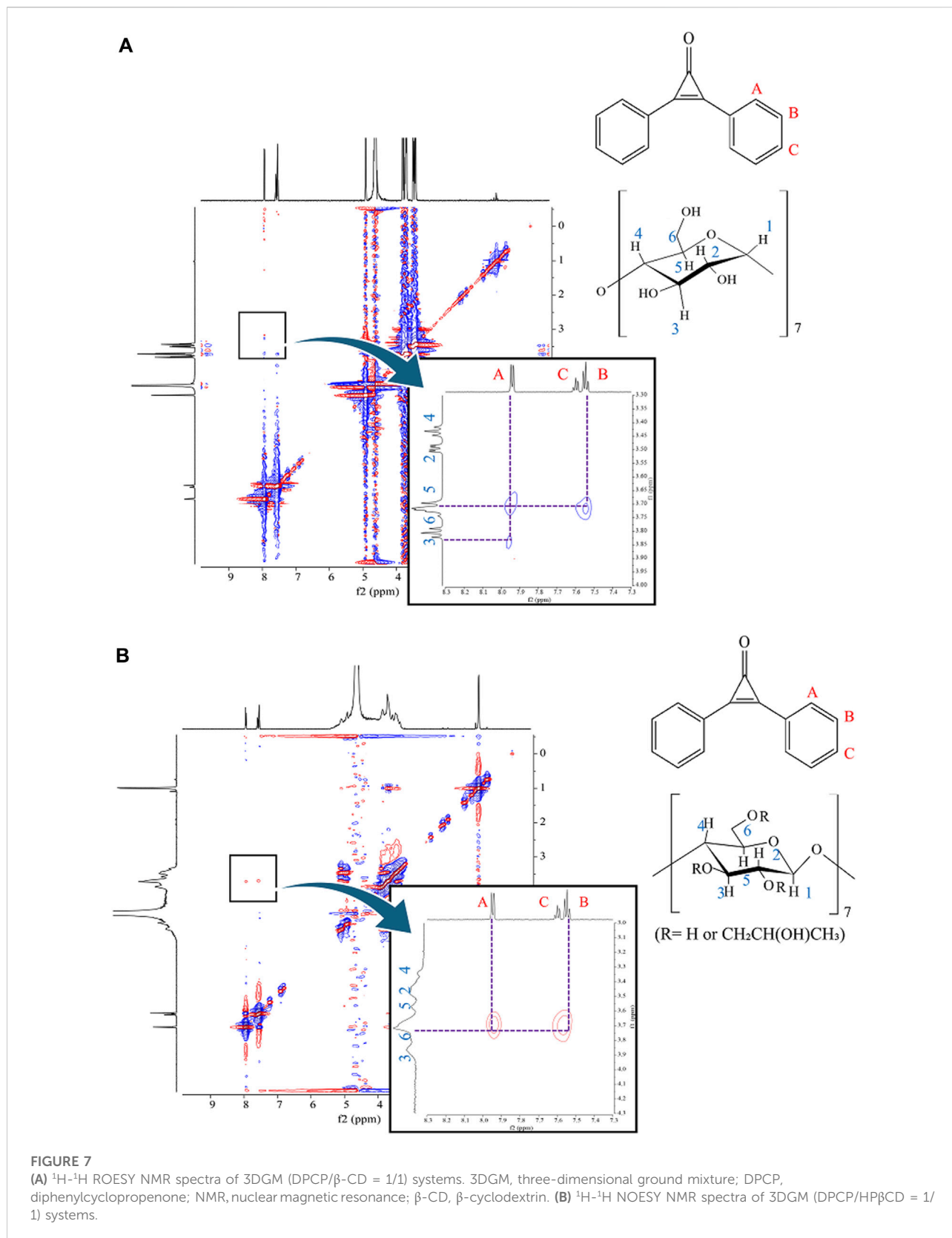
Measurement of IFN-γ in the culture medium

In this study, 3DGM samples indicated that DPCP/β-CD and DPCP/HPβCD form inclusion complexes at a

molar ratio of 1/1, albeit with distinct inclusion modes. DPCP is recognized for its ability to reduce elevated serum IFN-γ levels in patients with AA [34]. Thus, we investigated the anti-inflammatory effects of DPCP inclusion complexes (DPCP/β-CD and DPCP/HPβCD) using LPS-induced IFN-γ as a model to assess their efficacy (Figure 8).

The results demonstrated that DPCP alone significantly decreased LPS-induced IFN-γ levels at a concentration of 10^{-7} M compared to the control group. Conversely, β-CD and HPβCD alone did not show any effect on LPS-induced IFN-γ levels. Furthermore, both DPCP/β-CD and DPCP/HPβCD inclusion complexes significantly attenuated LPS-induced IFN-γ at a DPCP concentration of 10^{-7} M compared to the control group. Particularly, HPβCD/DPCP exhibited a more pronounced reduction in LPS-induced IFN-γ at lower concentrations (10^{-8} M), indicating a stronger inhibitory effect than that observed with DPCP alone or DPCP/β-CD. Additionally, the HPβCD group without encapsulated DPCP did not influence the LPS-induced IFN-γ levels.

These findings underscore that DPCP/β-CD and DPCP/HPβCD exert differential effects on reducing LPS-induced IFN-γ levels. The enhanced efficacy of HPβCD/DPCP suggests potential advantages in therapeutic applications aimed at mitigating conditions associated with elevated IFN-γ, such as AA.



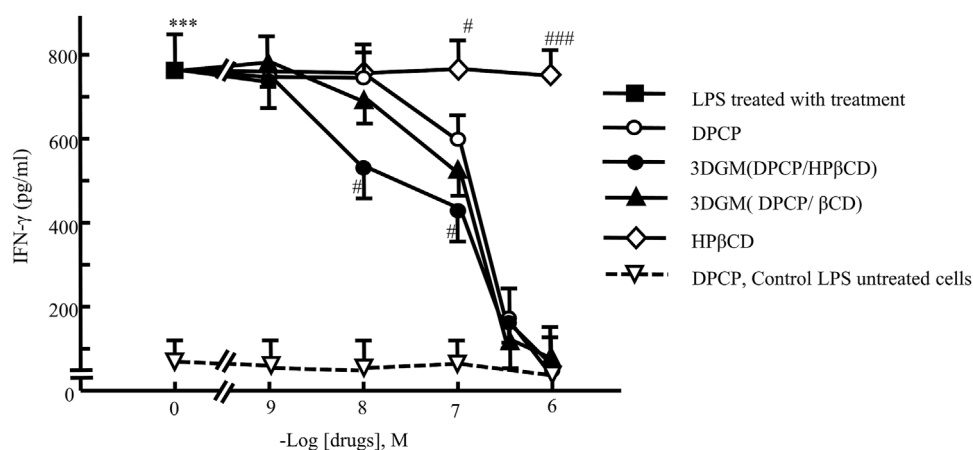


FIGURE 8

Dose-response relationship of DPCP and its inclusion compounds on LPS-induced IFN- γ secretion in primary cultured splenocytes: IFN- γ concentration (pg/ml) Cell seeding density: 5.0×10^5 cells/mL, data: means \pm standard errors of the mean (n = 3-4) ***($P < 0.001$) indicate significant differences from the control (medium alone) group, and #($P < 0.05$), ##($P < 0.01$) and ###($P < 0.01$) indicate significant differences from the LPS + DPCP group. DPCP, diphenylcyclopropanone; HP β CD, hydroxypropyl- β -cyclodextrin; LPS, lipopolysaccharide; NMR, nuclear magnetic resonance; β -CD, β -cyclodextrin.

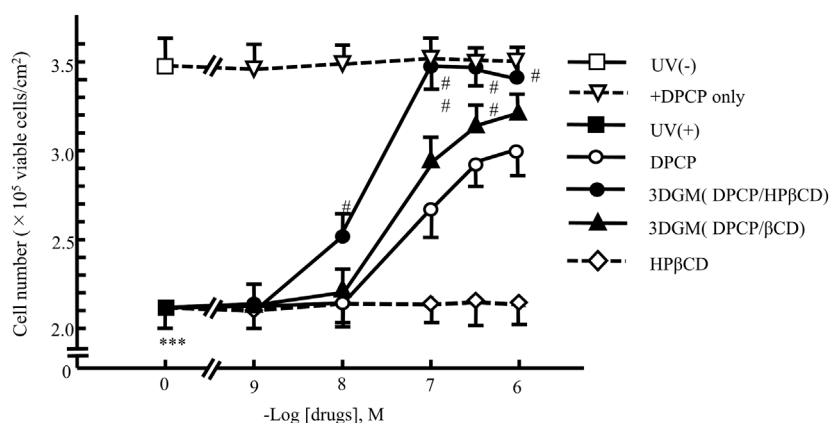


FIGURE 9

Dose-response relationship of DPCP and its inclusion compounds on UV-radiation-induced cell damage in NIH-3T3 cells cultured for 4 h Cell seeding density: 2.5×10^2 cells/cm², data: means \pm standard errors of the mean (n = 3-4) ***($P < 0.001$) indicate significant differences from the control [medium alone: UV (-)] group, and #($P < 0.05$) and ##($P < 0.01$) indicate significant differences from each UV (+)+DPCP group. DPCP, diphenylcyclopropanone; UV, ultraviolet.

Cell injury experiment

We investigated the protective effects of each drug on UV-irradiated NIH-3T3 cells subjected to UV damage (Figure 9). Following 4 h of UV irradiation, the number of viable NIH-3T3 cells decreased to approximately 70% compared to that of the untreated group (no UV irradiation, no drug added). In each drug-treated group, the decrease in cell viability was significantly attenuated in a dose-dependent manner.

The group supplemented with DPCP showed a dose-dependent suppression of UV-induced cell damage, with recovery to 85% of the non-UV-irradiated group observed at 10^{-6} M DPCP. Similarly, the β -CD/DPCP group, where DPCP was encapsulated in β -CD, exhibited a comparable protective effect against cell damage. In contrast, the HP β CD/DPCP group showed significant inhibition of cell damage starting from 10^{-8} M HP β CD/DPCP, with recovery to 97% of the non-UV-irradiated group at 10^{-7} M HP β CD/DPCP.

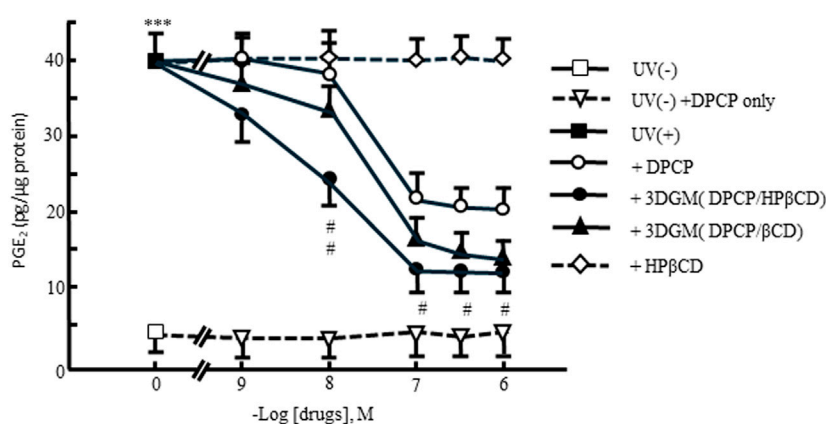


FIGURE 10

Dose-response relationship of DPCP and its inclusion compounds on UV-radiation-induced prostaglandin E₂ release in NIH-3T3 cells cultured for 4 h Cell seeding density: 2.5×10^2 cells/cm², data: means±standard errors of the mean (n = 3-4) ***($P < 0.001$) indicate significant differences from the control [medium alone: UV(-)] group, and #($P < 0.05$) and ##($P < 0.01$) indicate significant differences from each UV(+)+DPCP group. DPCP, diphenylcyclopropanone; UV, ultraviolet.

Furthermore, the release of PGE₂ into the culture medium of UV-irradiated NIH-3T3 cells after 4 h was evaluated (Figure 10). PGE₂ is a known chemical mediator involved in inflammation following UV radiation exposure. The addition of DPCP and its inclusion complexes led to a significant increase in PGE₂ release compared to the untreated group. However, DPCP and its complexes also showed a dose-dependent suppression of PGE₂ release induced by UV radiation. At 10^{-6} M DPCP, PGE₂ release was reduced to 50% of the UV-irradiated control, while β-CD inclusion and HPβCD groups exhibited inhibitory effects at lower concentrations. Notably, the HPβCD group at 10^{-7} M suppressed PGE₂ release to 25% of the UV-irradiated control, indicating a potent anti-inflammatory effect.

These results suggest that the addition of DPCP and its complexes protects UV-damaged NIH-3T3 cells, preserves cell viability, and reduces PGE₂ release, which is indicative of anti-inflammatory activity. The enhanced efficacy observed with HPβCD/DPCP compared to β-CD/DPCP may be attributed to differences in the inclusion modes of these complexes, highlighting the importance of inclusion complex formation in modulating biological activity.

The *ex vivo* cell studies aimed to validate whether inclusion complexes with β-CD derivatives could preserve the anti-inflammatory effects of DPCP. Results from these studies confirmed that both β-CD and HPβCD inclusion complexes maintained the anti-inflammatory properties of DPCP. Particularly noteworthy was the finding that the DPCP/HPβCD complex exhibited anti-inflammatory effects at lower concentrations compared to the DPCP/β-CD complex, which represents a novel discovery. This difference in inclusion modes, elucidated through NOESY NMR measurements, suggests a potential pharmacological advantage where DPCP demonstrates enhanced anti-inflammatory efficacy.

However, the safety and pharmacokinetic profiles of DPCP/β-CD inclusion complexes, which typically require comprehensive *in vivo* studies, remain a limitation of this research and should be addressed in future investigations.

The study unequivocally demonstrated that DPCP/β-CD complexes enhance solubility and retain anti-inflammatory properties. A clinical challenge highlighted is the current use of acetone, an organic solvent, in preparing DPCP for AA treatment. Based on these findings, future efforts will focus on scaling up the preparation method using 3D ball milling and exploring alternative formulation methods. Addressing the stability of DPCP/β-CD complexes in both solid-state and solution phases remains a critical challenge that requires further investigation.

As this study focused primarily on improving the solubility of DPCP, future research directions should include investigating skin permeability for potential clinical applications, thereby addressing the broader implications of these findings.

Conclusion

In this study, DPCP/β-CD and DPCP/HPβCD inclusion complexes were successfully prepared using the 3DGM method, which eliminates the need for organic solvents. Dissolution tests confirmed enhanced solubility of DPCP in both 3DGM (DPCP/β-CD = 1/1) and 3DGM (DPCP/HPβCD = 1/1) complexes. NMR analysis indicated that these complexes formed at a 1:1 molar ratio but exhibited distinct inclusion modes between DPCP/β-CD and DPCP/HPβCD. Notably, 3DGM (DPCP/HPβCD) demonstrated superior anti-inflammatory activity at lower doses compared to 3DGM (DPCP/β-CD), suggesting enhanced effectiveness of DPCP when complexed.

These findings hold promise for optimizing DPCP's handling characteristics and mitigating potential side effects. Improving DPCP's solubility through these complexes could expand its applications in various fields, including dermatology for treating conditions, such as AA. Moreover, this research underscores the importance of considering skin irritation potential in formulation development, crucial for ensuring patient safety and comfort.

By advancing the formulation of DPCP through innovative methods, such as 3D ball milling, this study enhances therapeutic efficacy and sets the stage for future clinical applications and formulation improvements.

Data availability statement

The original contributions presented in the study are included in the article/supplementary material, further inquiries can be directed to the corresponding author.

Ethics statement

The animal study was approved by the Institutional Animal Care and Use Committee of Josai University (Certification No. JU 23031). The study was conducted in accordance with the local legislation and institutional requirements.

Author contributions

Conceptualization, YI, KY, SK, and MK; methodology, KY and YI; software, YI, KY, SK, and MK; validation, YI, KY, SK, and MK; formal analysis, YI, KY, SK, HM, and MK; investigation, YI, KY, SK, MH, and MK; resources, YI, KY, and MK; data curation, YI, KY, and MK; writing—original draft preparation, YI, KY, and

MK; writing—review and editing, YI, KY, SK, NK, HM, and MK; visualization, YI, KY, and MK; supervision, YI and MK; project administration, YI, KY, SK, NK, HM, and MK; funding acquisition, YI and MK. All authors contributed to the article and approved the submitted version.

Funding

The author(s) declare that no financial support was received for the research, authorship, and/or publication of this article.

Acknowledgments

The authors are grateful to Cyclo Chem Bio Co., Ltd. for providing the cyclodextrin samples. The authors wish to thank the Instrument Analysis Center of Josai University for helpful advice on NMR spectroscopy. We thank the Laboratory of Nutri-Pharmacotherapeutics Management, Josai University, for their research support while taking measures against COVID-19 (SARS-CoV2) infection.

Conflict of interest

The authors declare that this study received β -cyclodextrin from Cyclo Chem Co., Ltd., which was not involved in the study design, collection, analysis, interpretation of data, the writing of this article or the decision to submit it for publication.

The remaining authors declare that the research was conducted in the absence of any commercial or financial relationships that could be construed as a potential conflict of interest.

References

- Hordinsky MK. Overview of alopecia areata. *J Invest Dermatol Symp Proc* (2013) 16(1):S13–15. doi:10.1038/jidsymp.2013.4
- Tanemura A, Oiso N, Nakano M, Itoi S, Kawada A, Katayama I. Alopecia areata: infiltration of Th17 cells in the dermis, particularly around hair follicles. *Dermatology* (2013) 226(4):333–6. doi:10.1159/000350933
- Waškiel-Burnat A, Osińska M, Salińska A, Blicharz L, Goldust M, Olszewska M, et al. The role of serum Th1, Th2, and Th17 cytokines in patients with alopecia areata: clinical implications. *Cells* (2021) 10(12):3397. doi:10.3390/cells10123397
- Lekhavit C, Rattanaumpawan P, Juengsamranphong I. Economic Impact of Home-Use versus office-use diphenylcyclopropanone in extensive alopecia areata. *Skin Appendage Disord* (2022) 8(2):108–17. doi:10.1159/000520568
- Kutlubay Z, Sevim Kecici A, Aydin O, Vehid S, Serdaroglu S. Assessment of treatment efficacy of diphenylcyclopropanone (DPCP) for alopecia areata. *Turk J Med Sci* (2020) 50(8):1817–24. doi:10.3906/sag-1807-230
- Tiwary AK, Mishra DK, Chaudhary SS. Comparative study of efficacy and safety of topical squaric acid dibutylester and diphenylcyclopropanone for the treatment of alopecia areata. *North Am J Med Sci* (2016) 8(6):237–42. doi:10.4103/1947-2714.185029
- Loftsson T, Brewster ME. Cyclodextrins as functional excipients: methods to enhance complexation efficiency. *J Pharm Sci* (2012) 101(9):3019–32. doi:10.1002/jps.23077
- Loftsson T, Duchêne D. Cyclodextrins and their pharmaceutical applications. *Int J Pharmaceutics* (2007) 329(1–2):1–11. doi:10.1016/j.ijpharm.2006.10.044
- Bezerra FM, Lis MJ, Firmino HB, Dias da Silva JG, Curto Valle RCS, Borges Valle JA, et al. The role of β -cyclodextrin in the textile industry—review. *Molecules* (2020) 25(16):3624. doi:10.3390/molecules25163624
- Mahalapbutr P, Wonganan P, Charoenwongpaiboon T, Prousoontorn M, Chavasiri W, Rungrotmongkol T. Enhanced solubility and anticancer potential of mansonone G by β -cyclodextrin-based host-guest complexation: a computational and experimental study. *Biomolecules* (2019) 9(10):545. doi:10.3390/biom9100545
- Michalska P, Wojnicz A, Ruiz-Nuño A, Abril S, Buendia I, León R. Inclusion complex of ITH12674 with 2-hydroxypropyl- β -cyclodextrin: preparation, physical characterization and pharmacological effect. *Carbohydr Polym* (2017) 157:94–104. doi:10.1016/j.carbpol.2016.09.072
- Hirayama F, Kurihara M, Uekama K. Improving the aqueous stability of prostaglandin E2 and prostaglandin A2 by inclusion complexation with

- methylated- β -cyclodextrins. *Chem Pharm Bull* (1984) 32(10):4237–40. doi:10.1248/cpb.32.4237
13. Shah M, Shah V, Ghosh A, Zhang Z, Minko T. Molecular inclusion complexes of β -cyclodextrin derivatives enhance aqueous solubility and cellular internalization of paclitaxel: preformulation and *in vitro* assessments. *J Pharm Pharmacol (Los Angel)* (2015) 2(2):8. doi:10.13188/2327-204X.1000011
14. Huang PH, Hu SCS, Yen FL, Tseng CH. Improvement of skin penetration, antipollutant activity and skin hydration of 7,3',4'-trihydroxyisoflavone cyclodextrin inclusion complex. *Pharmaceutics* (2019) 11(8):399. doi:10.3390/pharmaceutics11080399
15. Gamboa-Arancibia ME, Caro N, Gamboa A, Morales JO, González Casanova JE, Rojas Gómez DM, et al. Improving lurasidone hydrochloride's solubility and stability by higher-order complex formation with hydroxypropyl- β -cyclodextrin. *Pharmaceutics* (2023) 15(1):232. doi:10.3390/pharmaceutics15010232
16. Kang JH, Lee JE, Jeong SJ, Park CW, Kim DW, Weon KY. Design and optimization of rivaroxaban-cyclodextrin-polymer triple complex formulation with improved solubility. *Drug Des Dev Ther* (2022) 16:4279–89. doi:10.2147/DDDT.S389884
17. Bayomi MA, Abanumay KA, Al-Angary AA. Effect of inclusion complexation with cyclodextrins on photostability of nifedipine in solid state. *Int J Pharmaceutics* (2002) 243(1–2):107–17. doi:10.1016/s0378-5173(02)00263-6
18. Thaya R, Malaikozhundan B, Vijayakumar S, Sivakamavalli J, Jeyasekar R, Shanthi S, et al. Chitosan coated Ag/ZnO nanocomposite and their antibiofilm, antifungal and cytotoxic effects on murine macrophages. *Microb Pathogenesis* (2016) 100:124–32. doi:10.1016/j.micpath.2016.09.010
19. Saidman E, Chattah AK, Aragón L, Sancho M, Camí G, Garneró C, et al. Inclusion complexes of β -cyclodextrin and polymorphs of mebendazole: physicochemical characterization. *Eur J Pharm Sci* (2019) 127:330–8. doi:10.1016/j.ejps.2018.11.012
20. Shiozawa R, Inoue Y, Murata I, Kanamoto I. Effect of antioxidant activity of caffeic acid with cyclodextrins using ground mixture method. *Asian J Pharm Sci* (2018) 13(1):24–33. doi:10.1016/j.ajps.2017.08.006
21. 3D Ball Mill (3D Reactor). *Nagao system*. Inc. (2020). Available from: <https://www.nagaosystem.co.jp/> (Accessed March 4, 2020).
22. Inoue Y, Osada M, Murata I, Kobata K, Kanamoto I. Evaluation of solubility characteristics of a hybrid complex of components of soy. *ACS Omega* (2019) 4(5):8632–40. doi:10.1021/acso.9b00733
23. Higuchi T, Connors KA. Phase solubility techniques. *Adv Anal Chem Instrum* (1965) 4:117–212.
24. Jainchill JL, Aaronson SA, Todaro GJ. Murine sarcoma and leukemia viruses: assay using clonal lines of contact-inhibited mouse cells. *J Virol* (1969) 4(5):549–53. doi:10.1128/JVI.4.5.549-553.1969
25. Sakuma K, Ogawa M, Kimura M, Yamamoto K, Ogihara M. Inhibitory effects of shimotsu-to, a traditional Chinese herbal prescription, on ultraviolet radiation-induced cell damage and prostaglandin E2 release in cultured Swiss 3T3 cells. *Yakugaku Zasshi* (1998) 118(6):241–7. doi:10.1248/yakushi1947.118.6_241
26. Nelson SL, Hynd BA, Pickrum HM. Automated enzyme immunoassay to measure prostaglandin E2 in gingival crevicular fluid. *J Periodontol Res* (1992) 27(2):143–8. doi:10.1111/j.1600-0765.1992.tb01816.x
27. Loftsson T, Sigurdsson HH, Jansook P. Anomalous properties of cyclodextrins and their complexes in aqueous solutions. *Materials (Basel)* (2023) 16(6):2223. doi:10.3390/ma16062223
28. Iwata M, Fukami T, Kawashima D, Sakai M, Furuishi T, Suzuki T, et al. Effectiveness of mechanochemical treatment with cyclodextrins on increasing solubility of glimepiride. *Pharmazie* (2009) 64(6):390–4. doi:10.1691/ph.2009.9045
29. Inoue Y, Watanabe S, Suzuki R, Murata I, Kanamoto I. Evaluation of actarit/ γ -cyclodextrin complex prepared by different methods. *J Incl Phenom Macrocycl Chem* (2015) 81:161–8. doi:10.1007/s10847-014-0445-z
30. Naeem A, Yu C, Zang Z, Zhu W, Deng X, Guan Y. Synthesis and evaluation of rutin-hydroxypropyl β -cyclodextrin inclusion complexes embedded in xanthan gum-based (HPMC-g-AMPS) hydrogels for oral controlled drug delivery. *Antioxidants (Basel)* (2023) 12(3):552. doi:10.3390/antiox12030552
31. Tárkányi G, Németh K, Mizsei R, Tóke O, Visy J, Simonyi M, et al. Structure and stability of warfarin-sodium inclusion complexes formed with permethylated monoamino- β -cyclodextrin. *J Pharm Biomed Anal* (2013) 72:292–8. doi:10.1016/j.jpba.2012.09.003
32. Del Valle EMM. Cyclodextrins and their uses: a review. *Process Biochem* (2004) 39:1033–46. doi:10.1016/S0032-9592(03)00258-9
33. Tachikawa R, Saito H, Moteki H, Kimura M, Kitagishi H, Arce F, Jr, et al. Preparation, characterization, and *in vitro* evaluation of inclusion complexes formed between S-allylcysteine and cyclodextrins. *ACS Omega* (2022) 7(35):31233–45. doi:10.1021/acso.2c03489
34. Nowicka D, Maj J, Jankowska-Konsur A, Hrynczewicz-Gwózdź A. Efficacy of diphenylcyclopropanone in alopecia areata: a comparison of two treatment regimens. *Adv Dermatol Allergol* (2018) 35(6):577–81. doi:10.5114/ada.2018.77608